19th International Free-electron Laser Conference, Beijing, China, Aug. 18 ~ 22, 1997

The Physics Experiment for a Laser-driven Electron Accelerator

Y.C. Huang[1], *T. Plettner, R.L. Byer, R.H. Pantell*
Edward L. Ginzton Laboratory, Stanford University,
Stanford, CA 94305-4085

R.L. Swent, T.I. Smith
Hansen Experimental Physics Laboratory, Stanford University
Stanford, CA 94305

J.E. Spencer, R.H. Siemann, H. Wiedemann
Stanford Linear Accelerator Center
Stanford, CA 94305

Abstract - A physics experiment for laser-driven, electron acceleration in a structure-loaded vacuum is being carried out at Stanford University. The experiment is to demonstrate the linear dependence of the electron energy gain on the laser field strength. The accelerator structure, made of dielectric, is semi-open, with dimensions a few thousand times the laser wavelength. The electrons traverse the axis of two crossed laser beams to obtain acceleration within a coherence distance. We predict that the demonstration experiment will produce a single-stage, electron energy gain of 300 keV over a 2.5 mm distance. Ultimately, acceleration gradients of 1 GeV/m should be possible.

Keywords: laser, accelerator, free-electron laser
PACS: 29, 42.55.Tb

[1] Yen-Chieh Huang, Department of Nuclear Science, National Tsinghua University, Hsinchu, Taiwan 30043
email: ychuang@faculty.nthu.edu.tw, fax: 3-5718649, tel: 3-5715131 x 5525

I. Introduction

The demonstrated acceleration gradient of an RF accelerator is limited to ~ 100 MeV/m due to field emission from the copper cavity wall. At optical frequencies, the acceleration gradient can be enhanced by using dielectric materials for the accelerator structure. At 1 μm wavelength, a dielectric sustains 10-times higher damage fluence than copper[1]. With the rapid advance of laser technology, it appears that future accelerators driven by efficient diode-pumped solid-state lasers could meet the requirements for next generation high-gradient particle acceleration.

In addition to high gradient operation, a laser-driven accelerator should produce ultra-short electron bunches whose bunch length is several orders of magnitude shorter than those from an RF accelerator. The short electron bunch length, on the order of sub-femtosecond, is desirable for generating high power coherent radiation in single-pass type undulators. Recent theoretical studies on GeV-per-meter gradient, laser-driven electron accelerators have shown the potential for ultra-compact, table-top, free-electron lasers in the short wavelength range[2].

Two types of high gradient, laser-driven particle accelerators, structure-based and plasma-based, have been proposed. A structure-based laser-driven accelerator employs solid acceler istance between two adjacent accelerator cell boundaries is less than a π phase slippage distance or coherence distance. The accelerator cell length, scaled with the driving wavelength, is many orders of magnitude smaller than a conventional RF accelerator, but can be many times the driving laser wavelength. On the other hand, a plasma-based accelerator, which accelerates electrons using laser-excited, electrostatic waves inside a plasma, does not have solid boundaries.

For this type of accelerator, up to 100 GeV per meter acceleration gradient over a sub-millimeter distance has been experimentally demonstrated[3]. To become a practical device, the plasma-based accelerator has yet to demonstrate high-average-gradient acceleration over a macroscopic distance with a reasonable efficiency.

A structure-based accelerator, with a gradient limited by laser damage, employs direct laser fields to accelerate electrons in a relatively efficient fashion. A dielectric structure at optical frequencies sustains a higher damage threshold. For example, given a 1 μm wavelength and a 100 fsec laser pulse, the threshold damage field in dielectric materials like fused silica or magnesium fluoride is about 10 GV per meter[1]. The high damage threshold suggests the potential of GeV per meter average acceleration gradient by cascading a series of accelerator cells.

The laser-driven electron accelerator project, termed LEAP, is being carried out at Stanford University under a joint effort among the Edward Ginzton Laboratory, the Hansen Experimental Physics Laboratory (HEPL), and the Stanford Linear Accelerator Center (SLAC). The goal of the experiment is to verify linear electron acceleration from properly phased laser fields in a dielectric accelerator structure. The project is to set a theoretical and experimental foundation for future laser-driven particle accelerators. We report in the following the supporting theory, the experimental setup, and the predictions for the experiment.

II. Theory

Figure 1 illustrates the crossed-laser-beam acceleration scheme, where an electron is accelerated along the axis of the crossed laser fields. The two linearly polarized laser beams are phased such that the transverse fields cancel and the longitudinal fields add

along the electron axis. The insert defines the coordinate system used in this paper. The electron experiences the acceleration field until the optical phase slips ahead of the electron by π. The π phase slippage distance or the coherence distance is the maximum acceleration distance in an accelerator stage. A series of crossed laser beams can be arranged in successive dielectric boundaries to provide continuous acceleration. In our previous study, a 0.7 GeV per meter average gradient can be obtained by using a 1 μm wavelength pump laser operating at a 100 fsec laser pulse length. The accelerator cell length is 390 μm and the single stage energy gain is about 280 keV[4].

To demonstrate laser-driven acceleration, we selected a design that gives the maximum single-stage energy gain. For a highly relativistic electron moving along the *z* axis, the electron energy gain $\Delta W(z)$ along the electron direction *z* is given by[5]

$$\Delta W(\hat{z}) = 88\sqrt{P}\,\frac{1}{\hat{\theta}}\exp\left[-\frac{\hat{z}^2\hat{\theta}^2}{1+\hat{z}^2}\right]\sin\left[\frac{\hat{z}\hat{\theta}^2}{1+\hat{z}^2}\right], \qquad (1)$$

where *P* is the total laser power, $\hat{\theta} \equiv \theta/\theta_d$ is the laser crossing angle normalized to the laser far-field diffraction angle θ_d, $\hat{z} = z/z_r$ is the electron axial location *z* normalized to the optical Rayleigh range z_r, and *z* = 0 is chosen at the crossing point of the two laser beams. The maximum single stage energy gain $\Delta W_{\max} = 30\sqrt{P(\mathrm{TW})}$ MeV occurs at the crossing angle $\hat{\theta} = 1.37$ and the interaction length $2l = 0.92 z_r$ or $2\hat{l} = 0.92$ for the normalized coordinate[6]. The condition $\hat{\theta} = 1.37$ and $2\hat{l} = 0.92$ corresponds to a π phase slippage distance in a single accelerator stage. Given a Ti:sapphire laser operating at a 1 psec pulse length and 1 mJ per pulse, the maximum single stage energy gain for a highly relativistic beam is 0.67 MeV.

For a finite γ, the laser field along *z* seen by an on-axis electron is given by[4, 5]

$$E_z(z) = -2\sqrt{2\eta I_{\max}}\,\theta\frac{(1+\hat{l}^2)^{1/2}}{1+\hat{z}^2}\exp\left[-\frac{\hat{z}^2\hat{\theta}^2}{1+\hat{z}^2}\right]\cos\left[\frac{\hat{z}\hat{\theta}^2}{1+\hat{z}^2}+2\tan^{-1}\hat{z}+\frac{\hat{z}}{\theta_d^2\gamma^2}\right], \qquad (2)$$

where η is the wave impedance, $I_{\max}$ is the maximum laser intensity that can be tolerated by optical components located at $\hat{z} = \pm\hat{l}$. The maximum single-stage energy gain is the integration of the electric field over the π phase slippage distance. Figure 2 shows the single-stage energy gain and the maximum acceleration distance versus the electron injection energy γ with design parameters: $\hat{\theta} = 1.37$, $2\hat{l} = 0.92$, $I_{\max} = 5\,\mathrm{J/cm}^2$ for 1 psec laser pulses[1] and 1 GW laser power. Both the energy gain and the coherence distance, as expected, grow monotonically with γ. As the electron injection energy increases to several hundred MeV, the single stage energy gain converges to the predicted value, 0.67 MeV. The superconducting accelerator at the Stanford Hansen Experimental Physics Laboratory provides a beam energy of 35 MeV or γ = 70. At this energy the single-stage energy gain and the coherence distance are reduced from its maximum value by a factor of two to three.

The condition $\hat{\theta} = 1.37$ and $2\hat{l} = 0.92$ used in Fig. 2 may not maximize that for a finite injection energy. With a fixed laser intensity $I_{\max} = 5\,\mathrm{J/cm}^2$ for 1 psec laser pulses, the maximum acceleration distance $2l$ and the maximum single-stage energy gain $\Delta W_{\max}$ can be determined numerically from Eq. (2) by knowing the laser far-field diffraction angle and the laser crossing angle. Since the laser power $P_{\max} \approx 1$ GW and $I_{\max} = 5\,\mathrm{J/cm}^2$, the relationship $P_{\max} = I_{\max}\,\pi w(l)^2/2$ gives the laser spot size $w(l) = 80\,\mu\mathrm{m}$ at the optical component. As discussed in Refs. [1, 6], the laser field ought

to be terminated within a Rayleigh range, and therefore the laser spot size remains approximately a constant along the accelerator axis. To a good approximation, the laser waist at $z = 0$ is $w_0 \approx w(l) = 80$ μm. From the definition for the far-field diffraction angle $\theta_d \equiv \lambda/\pi w_0$, one obtains $\theta_d = 4$ mrad for a 1 μm laser wavelength. Given $I_{\max} = 5\,\mathrm{J/cm}^2$, $P_{\max} = 1$ GW, $\theta_d = 4$ mrad, and $\gamma = 70$, Fig. 3 shows the numerical results of the single-stage energy gain and the maximum acceleration distance versus the laser crossing angle. A large laser crossing angle causes more phase slip, which reduces both the energy gain and the coherence length. On the other hand, a small crossing angle reduces the acceleration field, but gives a better phase velocity matching. At the maximum single-stage energy gain 330 keV, the laser crossing angle is 13 mrad, and the corresponding maximum acceleration distance is 2.5 mm.

III. Experimental Setup

The Stanford Hansen Experimental Physics Laboratory provides both the electron injector and the pump laser for the LEAP experiment. The superconducting accelerator at the HEPL generates a 35 MeV electron beam at a 11.8 MHz micropulse repetition rate over a macropulse length of ~ 3 msec. Currently the electron macropulse is being upgraded from a 10 Hz repetition rate to a continuous wave mode. The electron beam parameters are: energy spread ≈ 0.1%, normalized emittance ≈ 8 π-mm-mrad, micropulse length ≈ 2 psec, and 10^8 electrons/micropulse. The mode-locked Ti:sapphire laser generates 0.1 ~ 1 picosecond laser pusles with a 1mJ/pulse energy at a 1 kHz repetition rate.

Figure 4 shows the experimental setup for demonstrating the laser-driven electron acceleration. The LEAP beam line is at the end of the HEPL FEL beam line. To

synchronize the Ti:sapphire laser to the electron pulse, the cross correlation signal of the Ti:sapphire laser and the FEL is fed back to a PZT that adjusts the Ti:sapphire laser cavity length. We assume that the FEL pulses are in synchronization with the electron pulses.

A "rogue" pulse at the Ti:sapphire laser repetition rate of 1 kHz is inserted between the regular 11.8 MHz electron pulses. The rogue pulse does not interact with the FEL and retains its original beam quality after the FEL wiggler. A fast kicker then deflects the rogue pulses to the LEAP experiment. The rogue pulse scheme permits the operation of the FEL for synchronization purpose while avoiding the background noise from 11.8 MHz regular pulses.

The laser optics at the interaction region is depicted in Fig. 5. Each Ti:sapphire laser pulse is split into two identical pulses in the Mach Zender beam splitter. The prism sliding in the horizontal direction provides adjustment for the relative phase between the crossed beams. The prism sliding in the vertical direction provides adjustment for the laser crossing angle.

The emittance filter is to remove the electrons that may not transit the accelerator stage for a given electron transit aperture. The acceptance is determined by the electron transit aperture size and the accelerator stage length. The aperture can be a rectangular shape with a long dimension in y. For an interaction length of 2.5 mm (see Fig. 3) and a rectangular aperture of $4\ \mu\text{m} \times 1$ mm, the acceptance is approximately 10^{-3} π-mm-mrad. Given a normalized emittance of 8 π-mm-mrad for the 35 MeV beam from the injector, approximately 1% of the whole electron beam or 10^9 electrons/sec interact with the laser beam, if a 1 kHz electron pulse repetition rate is assumed. Our study shows that a 4 μm

wide electron aperture in the accelerator reduces the single stage energy gain by 20% and a 6 μm one reduces the gain by 40%. The energy gain reduction is due to the laser field leaking from an aperture larger than the laser wavelength.

The maximum energy gain, as calculated in the last section, is about 330 keV, which is ~ 1% of the electron injection energy. An energy spectrometer with 10^{-4} resolution after the emittance filter allows the detection of ~ 1% energy modulation. The energy measurement will be carried out over a wide range of parameters, including laser power, laser crossing angle, laser waist size, interaction length, electron transit aperture size, and relative phase of the crossed laser beams.

IV. Summary

A physics experiment for demonstrating laser-driven electron acceleration is being carried out at Stanford University. The project is a joint effort among the Ginzton Laboratory, the Hansen Experimental Physics Laboratory, and the Stanford Linear Accelerator Center. The goal of the experiment is to achieve electron linear acceleration in a structure loaded vacuum. The accelerator, made of dielectric optical components, is driven by a mode-locked Ti:sapphire laser. We intend to measure the electron energy gain versus laser power, laser crossing angle, laser waist size , interaction length, electron transit aperture size, and relative phase of the crossed laser beams. The system parameters for the laser and the electron injector are listed in Table 1. The accelerator design parameters are summarized in Table 2.

The LEAP project is expected to demonstrate vacuum laser-driven electron acceleration in a semi-open dielectric structure that is a few thousand times larger than

the driving wavelength. The success of this project may, in the future, lead to efficient short-wavelength undulator radiation as well as to compact TeV-class linear colliders.

Acknowledgement

This work is supported by the U.S. Department of Energy under the contract DE-FG03-97ER41043. The work at SLAC is supported by the U.S. Department of Energy under the contract DE-AC03-76SF00515. We appreciate assistance from the Stanford Picosecond FEL Center, directed by Prof. H.A. Schwettman. We also thank M.T. Hennessy for helping the experimental setup.

Table 1 System parameters for the pump laser and the electron injector.

laser System	pulse width	energy/pulse	repetition rate	wavelength
mode-locked Ti:sapphire laser	0.1 ~ 3 psec	1 mJ	1 kHz	0.8 ~ 1 μm

electron injector	pulse width	energy	number of electrons	repetition rate	energy spread	normalized emittance
superconducting accelerator	~2 psec	35 MeV	10^8/pulse	< 1 kHz	0.1%	8 π-mm-mrad

Table 2 The accelerator design parameters for maximizing single-stage energy gain.

Laser crossing angle	laser far-field diffraction angle	laser power	electron energy gain	interaction length	accelerated electrons
13 mrad	4 mrad	1 GW	330 keV	2.5 mm	< 10^9/sec

Figure Captions:

Figure 1 The crossed-laser-beam electron acceleration scheme. The two linearly polarized laser beams are phased such that the transverse fields cancel and the longitudinal fields add along the electron axis. The insert defines the coordinate system used in this paper.

Figure 2 The dependence of the single-stage energy gain and the maximum acceleration length on the electron energy. For highly relativistic electrons, the maximum single-stage energy gain can be 0.67 MeV and the coherence distance can be 14 mm long. One GW laser power is assumed.

Figure 3 Single-stage energy gain and the maximum acceleration distance versus the laser crossing angle, subject to the system parameters $I_{\max} = 5\,\mathrm{J/cm}^2$, $P_{\max} = 1$ GW, $\theta_d = 4$ mrad, and $\gamma = 70$. A large laser crossing angle causes more phase slippage, which reduces both the energy gain and the coherence length. On the other hand, a small crossing angle reduces acceleration field, but gives a better phase velocity matching.

Figure 4 Experimental setup for the LEAP experiment. The synchronization between the Ti:sapphire laser and the electron pulse is provided by the sum frequency generation of the FEL and the Ti:sapphire laser mixed in a $AgGaSe_2$. The rogue pulse at 1 kHz, unaffected by the FEL, is deflected into the interaction chamber by using a fast deflector.

Figure 5 The optical configuration at the interaction region. Each Ti:sapphire laser pulse is split into two identical ones at the Mach Zhender beam splitter. The prism, sliding in the horizontal direction, is to provide adjustments for the relative

phase between the two pulses. The prism, sliding in the vertical direction, is to provide adjustments for the laser crossing angle. The emittance filter collimates electrons.

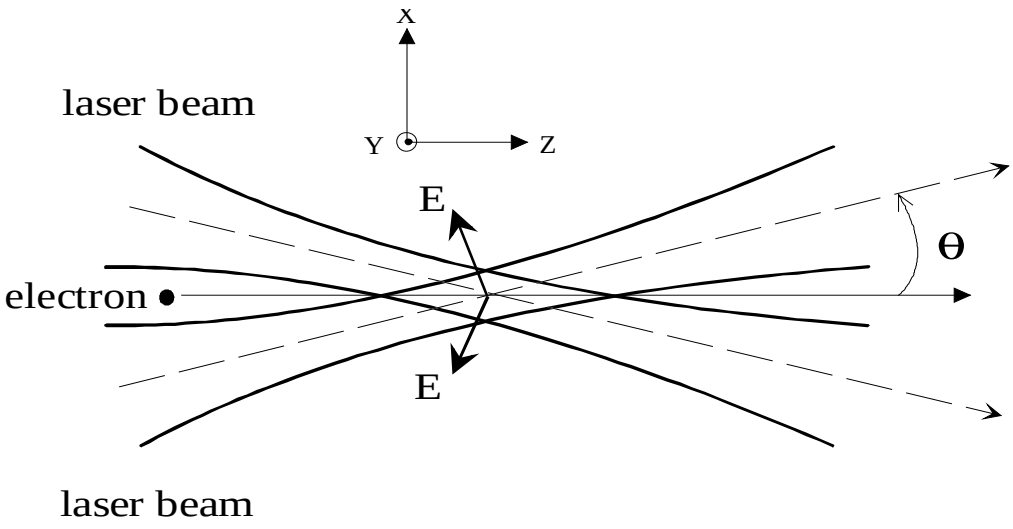

Figure 1

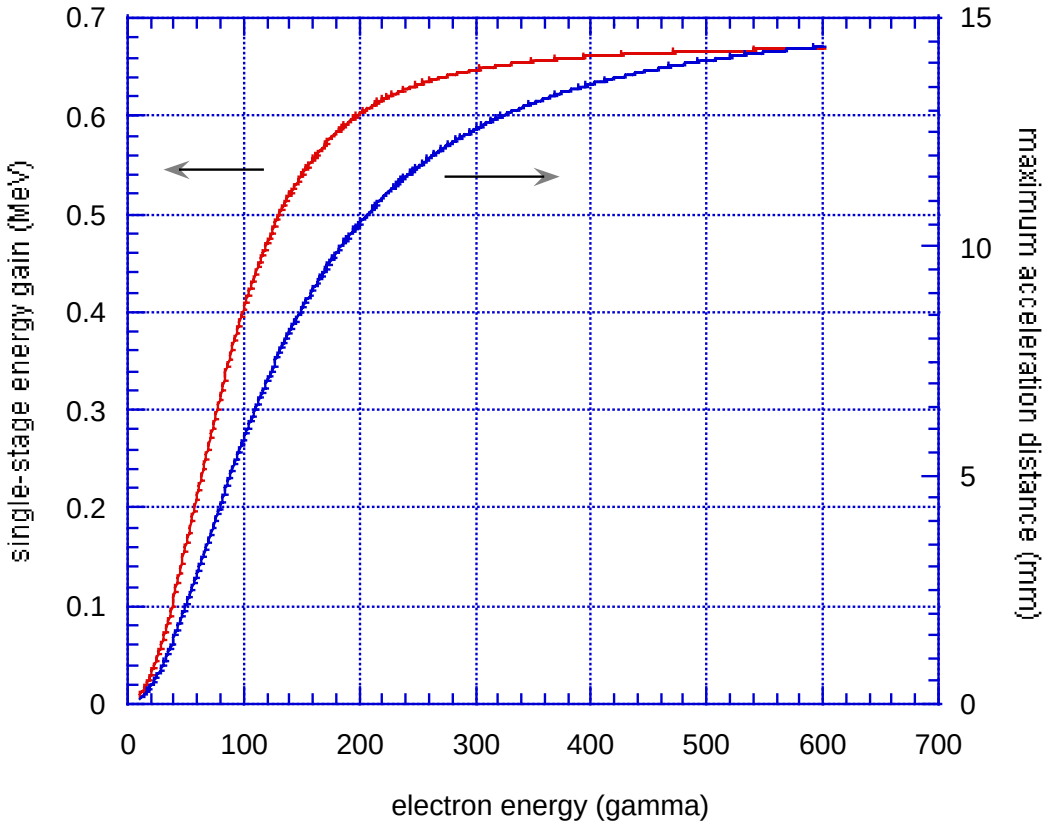

Figure 2

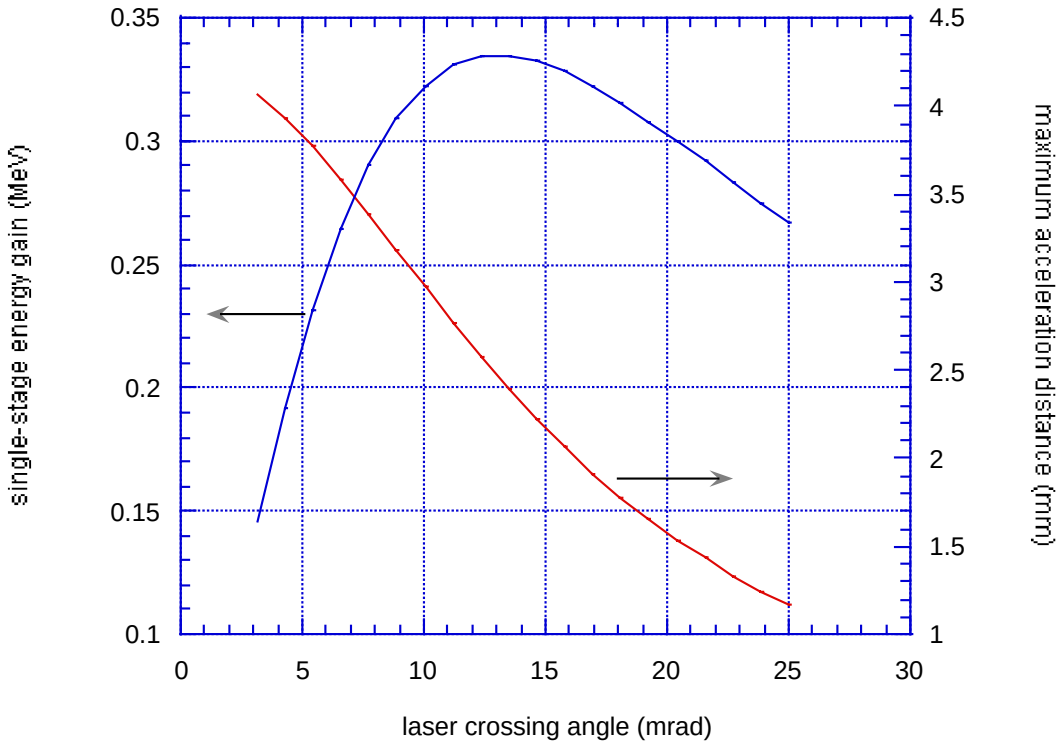

Figure 3

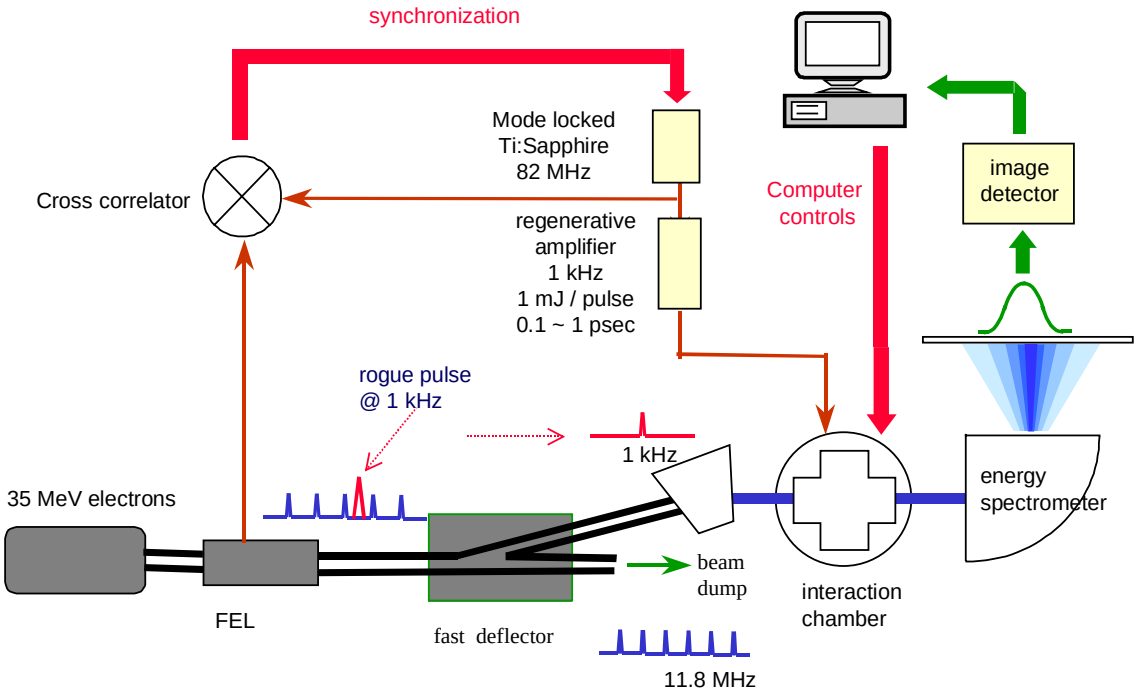

Figure 4

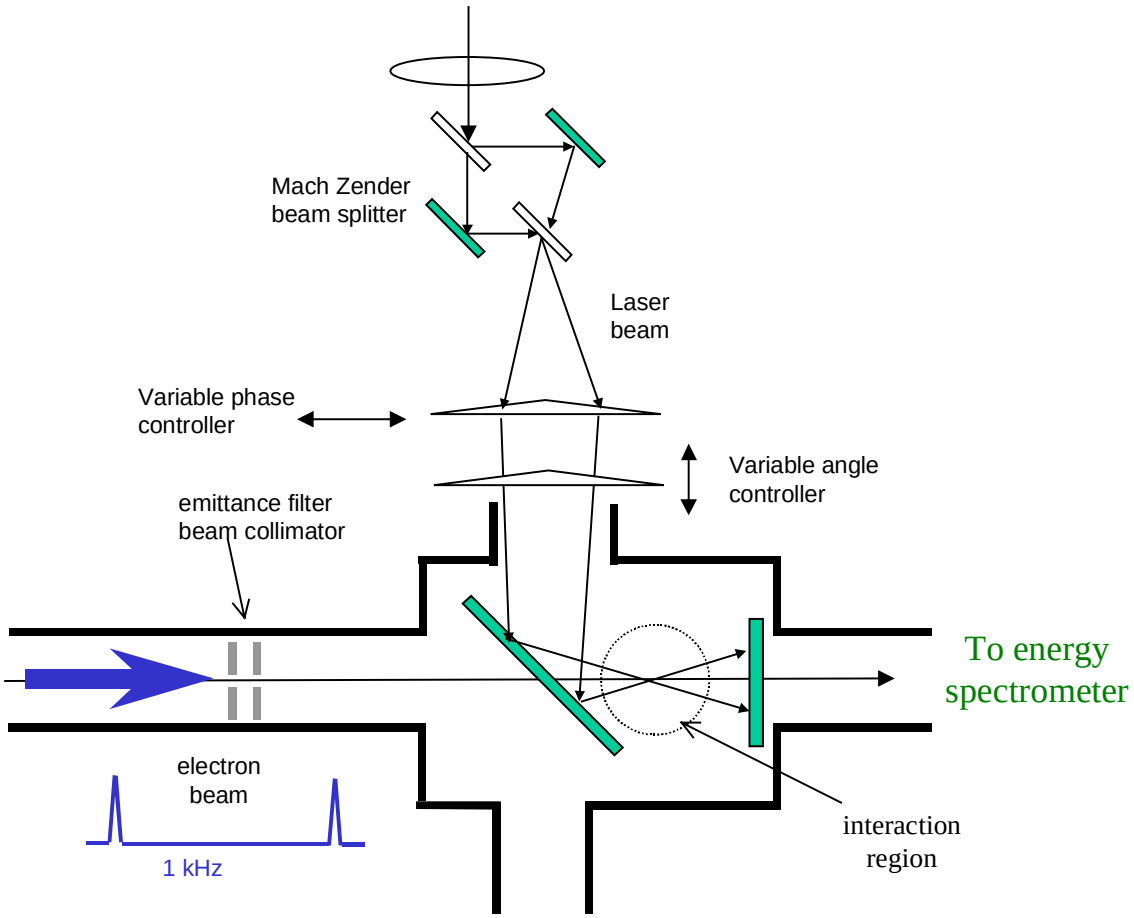

Figure 5

---

[1] Y.C. Huang and R.L. Byer, Proceedings of the Symposium on Generation, Amplification, and Measurement of Ultrashort laser pulsese III, 28-30 Jan., 1996, San Jose CA, SPIE Vol. 2701, pp. 210~219.

[2] Y.C. Huang and R.L. Byer, in Proceedings of the 18th International Free-electron Laser Conference, 26 ~ 30 Aug., 1996, Rome, Italy.

[3] C. E. Clayton et al and K. Nakajima et al to be published in the proceedings of the Advanced Accelerator Concepts Workshop, Lake Tahoe, 1996 (AIP, NY, 1997), S. Chattopadhay editor.

[4] Y.C. Huang and R.L. Byer, *Appl. Phys. Lett.* **69** (15), 7 Oct, 1996, pp. 2175~2177.

[5] P. Sprangle, E. Esarey, J. Krall, A. Ting, *Optical Comm.* 124, 1996, pp. 69~73.

[6] Y.C. Huang, D. Zheng, W.M. Tulloch, and R.L. Byer, *Appl. Phys. Lett.* **68** (6), 5 Feb., 1996, pp. 753~755.